



Partially compromised specification causes stochastic effects on gut development in *C. elegans*



Hailey Choi^{a,b}, Gina Broitman-Maduro^a, Morris F. Maduro^{a,*}

^a Department of Biology, University of California, Riverside, CA 92521, United States

^b Graduate program in Cell, Molecular and Developmental Biology, University of California, Riverside, CA 92521, United States

ARTICLE INFO

Keywords:

C. elegans
Endoderm
Cell specification
Robustness
Gene regulatory networks
Morphogenesis
Hyperplasia

ABSTRACT

The *C. elegans* gut descends from the E progenitor cell through a series of stereotyped cell divisions and morphogenetic events. Effects of perturbations of upstream cell specification on downstream organogenesis have not been extensively investigated. Here we have assembled an allelic series of strains that variably compromise specification of E by perturbing the activation of the gut-specifying *end-1* and *end-3* genes. Using a marker that allows identification of all E descendants regardless of fate, superimposed with markers that identify cells that have adopted a gut fate, we have examined the fate of E lineage descendants among hundreds of embryos. We find that when specification is partially compromised, the E lineage undergoes hyperplasia accompanied by stochastic and variable specification of gut fate among the E descendants. As anticipated by prior work, the activation of the gut differentiation factor *elt-2* becomes delayed in these strains, although ultimate protein levels of a translational ELT-2::GFP reporter resemble those of the wild type. By comparing these effects among the various specification mutants, we find that the stronger the defect in specification (i.e. the fewer number of embryos specifying gut), the stronger the defects in the E lineage and delay in activation of *elt-2*. Despite the changes in the E lineage in these strains, we find that supernumerary E descendants that adopt a gut fate are accommodated into a relatively normal-looking intestine. Hence, upstream perturbation of specification dramatically affects the E lineage, but as long as sufficient descendants adopt a gut fate, organogenesis overcomes these effects to form a relatively normal intestine.

1. Introduction

Organogenesis is an essential part of metazoan development. During this process, progenitor cells activate gene regulatory networks to drive specification, regulate mitotic divisions, direct cell migration and morphogenesis to form the appropriate shape of an organ or tissue, and activate terminal tissue-specific genes. In the face of sources of gene expression variation, robustness of organ formation is generally assured by several mechanisms. Embryonic gene networks include feed-forward and autoregulatory loops that enforce downstream gene activation and maintain cell identity (Davidson, 2010). Organ size can be regulated by global and local mechanisms that influence cell proliferation and cell size (Hariharan, 2015; Irvine and Harvey, 2015; Patel et al., 2017). Experimental perturbations of the earliest steps in organ specification, therefore, might not always have consequences for later organ development, depending on the extent to which compensatory mechanisms can overcome their effects.

In the nematode *C. elegans*, embryonic patterning must be especially robust because the animal lacks compensatory mechanisms

to replace missing somatic cells. In particular, the gut (intestine) is clonally generated from a single embryonic cell called E (Fig. 1A). In wild-type animals, the E cell undergoes a stereotyped pattern of cell divisions to produce 20 (and rarely, 21 or 22) cells that form the larval intestine (Fig. 1B; Sulston et al., 1983). During embryogenesis, the developing gut primordium undergoes morphogenesis in a highly reproducible way with only minor animal-to-animal variation (Asan et al., 2016). Because the E founder cell generates only one tissue, and development occurs in a highly predictable way from one embryo to the next, the intestine has been a good model for investigating the relationship among specification, cell fate and the cell lineage (Boeck et al., 2011; Maduro, 2017; Sulston et al., 1983).

The gene regulatory network that drives E specification has been a focus of study for more than 25 years (Fig. 1C). The most critical zygotic regulators for specifying gut are the paralogous and redundant END-1 and END-3 GATA transcription factors, as loss of both genes together results in a complete failure to specify endoderm (Maduro et al., 2005a; Owrighi et al., 2010). The absence of gut is sometimes compatible with normal development of the rest of the embryo,

* Corresponding author.

E-mail address: mmaduro@ucr.edu (M.F. Maduro).

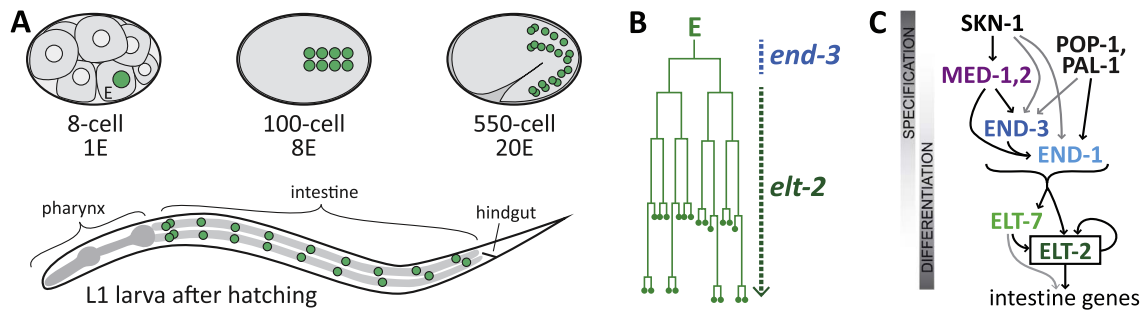


Fig. 1. Endoderm specification and E lineage development. (A) The locations of the E lineage nuclei at various stages in normal development, modified from (Maduro, 2015). Overall embryogenesis takes ~12 h at 25 °C (Sulston et al., 1983). (B) Cell division pattern of the wild-type E progenitor cell, after (Sulston et al., 1983). The vertical axis is time and a horizontal line indicates a cell division. The approximate time of transcription of *end-3* and *elt-2* is shown to the right of the diagram. (C) Simplified pathway showing hierarchy of transcription factors, modified from (Maduro, 2015). The endoderm specification strains described in this work perturb the overall contributions made by the MED-1,2 and END-1,3 regulators in a way that does not affect other lineages. Embryos are ~50 μm long and the larva is ~200 μm long. Dorsal is at top and anterior is to the left.

resulting in a larva with an absent gut but relatively normal morphogenesis (Maduro, 2009; Owraghi et al., 2010). Normal expression of the *end* genes occurs in the early E lineage, but only transiently, as their primary function is to activate expression of *elt-2* and *elt-7*. Expression of *elt-2* and *elt-7* is then maintained by positive autoregulation throughout the remainder of development and adulthood (Fukushige et al., 1998; Sommermann et al., 2010). ELT-2 is the predominant factor maintaining intestinal fate, as loss of *elt-2* alone results in embryos that contain a malformed gut, while loss of *elt-7* alone has no apparent phenotype though its loss can synergize with loss of *elt-2* (Fukushige et al., 1998; Sommermann et al., 2010). All four of END-1, END-3, ELT-2 and ELT-7 form a group of 'endodermal GATA factors' that have similar transcription factor activities, in that any of one of them is sufficient to specify the gut when overexpressed ectopically, and ELT-2 under the control of the *end-1* promoter can even specify gut in the E lineage in the absence of the other three genes (Du et al., 2016; Maduro et al., 2005a; Sommermann et al., 2010; Wiesenfahrt et al., 2015; Zhu et al., 1998). Parallel maternal and zygotic inputs upstream of END-1, END-3, ELT-2 and ELT-7 contribute to timely activation of *end-1* and *end-3* in the early E lineage (Maduro et al., 2005b, 2001; Shetty et al., 2005). These upstream factors are also required for specification of other early embryonic cells, hence their perturbation results in embryos that arrest with abnormal morphogenesis (Bowerman et al., 1992; Hunter and Kenyon, 1996; Lin et al., 1995).

An important question in development is how developing embryos cope with the stochastic nature of gene expression. Expression variation due to intrinsic and extrinsic factors occurs in many systems (Blake et al., 2003; Colman-Lerner et al., 2005; Holloway et al., 2011; Raj et al., 2010). The branched, redundant architecture of the zygotic gut specification network in *C. elegans* makes gut specification robust, but it also allows the construction of strains that have partial defects in gut specification in which the inherent variability of gene expression becomes apparent (Maduro et al., 2015, 2007). In such backgrounds, which we call "Hypomorphic Gut Specification" or HGS strains, gut development becomes highly stochastic: The number of gut nuclei that are made, as identified by expression of an *elt-2*::GFP transcriptional reporter, varies from none to over 30 (Maduro et al., 2015, 2007). We have interpreted these results to mean that gut specification is not strictly an all-or-none phenomenon at the level of the E blastomere, and proposed that the variable number of gut nuclei in HGS embryos is likely to be the result of two effects occurring simultaneously: One is an increase in the number of cells made by E, and the other is a stochastic adoption of gut fate among those descendants (Maduro, 2015).

Here, we examine gut specification mutant strains for their effect on the E lineage, from mid- to late embryogenesis. We use a two-reporter strategy that allows us to visualize, at any embryonic stage, all descendants of the E cell as well as those E descendants that have committed to a gut fate. We find that all HGS strains produce extra cell

divisions within the E lineage, and that the stronger the defect in gut specification, the lower the proportion of cells that commit to a gut fate. Surviving HGS adults have more similar numbers of gut nuclei across all HGS strains, consistent with a required minimum number of gut cells for survival past the first larval stage. We find that expression of the terminal regulator ELT-2 is delayed in HGS embryos, proportional to the severity of the specification defect, but that final levels of ELT-2 expression are essentially normal. Finally, using a marker that enables visualization of cell membranes in the gut primordium, we find that the developing gut can accommodate extra cells produced by the E lineage, both in HGS strains as well as in a previously described mutant that dramatically increases cell divisions with the E lineage without affecting cell specification. Together, these results show that timely activation of gut specification is critical for establishing the correct pattern of cell divisions within the E lineage and the full commitment of all E descendants to an intestinal fate. We also find that variability in the pattern of cell divisions with the E lineage can be accommodated during gut development, as long as sufficient E descendants adopt a gut fate.

2. Materials and methods

2.1. Strains and worm handling

The wild-type control was N2. All strains were grown on *E. coli* OP50 and maintained at 20–22 °C and observed at 23–25 °C except as noted. Mutations and transgenes were as follows. *LG I: cdc-25.1(rr31), irSi10 [end-3(MED sites mutated) + Cb-unc-119], irSi13 [end-3(+) + Cb-unc-119(+)]*. *LG II: irSi7 [end-1(MED sites mutated), Cb-unc-119(+)], irSi9 [end-1(+), Cb-unc-119(+)], irSi12 [end-1,3(+), Cb-unc-119(+)]*. *LG III: med-2(cxTi9744)*. *LG IV: him-8(e1489), him-8(me4), irIs98 [Cb-unc-119(+), end-1(MED sites mutated), end-3(MED sites mutated), irSi24 [pept-1/opt-2::mCherry::H2B, Cb-unc-119(+)], itIs37 [Cb-unc-119(+), pie-1::H2B::mCherry]*. *LG V: end-1(ok558), end-3(ok1448), end-3(ir62), end-3(ir64), oxTi389 [Cb-unc-119(+), eft-3::H2B::dTomato], stIs10116 [Cb-unc-119(+), his-72::H2B::mCherry], zuls70 [end-1::GFP::CAAX], irIs133 [elt-2::mCherry::H2B, unc-119::CFP, rol-6D]*. *LG X: med-1(ok804), rrIs1 [unc-119(+), elt-2::NLS::GFP::lacZ], wIs84 [rol-6D, elt-2::NLS::GFP::lacZ]*. Unmapped: *stIs10064 [Cb-unc-119(+), end-3::HIS-24::mCherry::let-858_3'UTR], gals290 [elt-2::ELT-2::TY1::EGFP::3xFLAG]*. Extrachromosomal arrays: *irEx697 [elt-2::mCherry::H2B, unc-119::CFP, rol-6D]*. Mutations and transgenes were combined using standard crosses. The *cdc-25.1(rr31)* strain was grown at 23–25 °C. Because of the close proximity of *zuls70* to *end-3* (< 2 map units), we made a *de novo* null mutation (*ir64*) in *end-3* in a *zuls70* strain using CRISPR/Cas9-mediated mutagenesis (Arriberre et al., 2014) with guide RNAs with targeting regions 5'-aacacgtgaatttagag-3' and 5'-tcgggaacgaattgtgg-3', which delete 1.1 kbp of the *end-3*

locus including its promoter and most of the END-3 coding region. The *ir64* lesion is identical to that of *ir62* which was made in an N2 background (strain MS2267). Mutations in *him-8* were used to generate males, and the resulting strains were confirmed to be lacking *him-8* by the absence of males over several generations. To facilitate recovery of some strains, mapped transgene insertions were used as counter-selection markers. Recovery of strains was confirmed by PCR, reporter expression and/or expected phenotype. Some strains may carry a background *unc-119* mutation whose phenotype is rescued by the presence of one or more integrated transgenes carrying *unc-119(+)*.

2.2. Construction of specification-compromised strains

Endoderm specification strains are listed in Table 1. Construction of MS1762, MS1763, MS1809, and MS1810 was described previously (Maduro et al., 2015). MS1548 was produced as follows. Plasmid pMM869 was constructed, which carries *Cb-unc-119(+)* and the *end-1* and *end-3* genes with mutations in the MED binding sites as described (Maduro et al., 2015). pMM869 was integrated into the genome by microparticle bombardment of an *unc-119(ed4)* strain (Praitis et al., 2001). The resulting integrated line was crossed into an *unc-119(ed4); end-1(ok558) end-3(ok1448); Ex[end-3(+), sur-5::dsRed]* strain and F₂ progeny were obtained that failed to segregate Unc and which lacked the *end-3(+)* array. The resulting strain, *end-1(ok558) end-3(ok1448); unc-119(ed4); irIs98* was saved as MS1548. We note that both the MS1548 and MS404 strains, and others derived from them, exhibit a tendency to undergo a phenotypic suppression after several months of

Table 1

A set of zygotic endoderm specification strains of varying severity.

Strain	Genotype	Embryos making gut ^a	Viability ^b
E(100) / N2	wild type	100% (n > 500) (control)	100% (n > 200)
E(100) / MS1810 ^c	<i>end-1(ok558) end-3(ok1448); Si[end-1(+)]; Si[end-3(+)]</i>	100% (> 500) (control)	100% (n > 200)
E(95) / RB1331	<i>end-3(ok1448)</i>	96% (221)	81% (140)
E(95) / MS2267	<i>end-3(ir62)</i>	95% (232)	n.d.
E(75) / MS1809 ^c	<i>end-1(ok558) end-3(ok1448); Si[end-1(MED-)]; Si[end-3(MED-)]</i>	75% (459)	42% (120)
E(50) / MS1548	<i>end-1(ok558) end-3(ok1448); irIs98 [end-1(MED-), end-3(MED-)]</i>	48% (143)	39% (140)
E(40) / MS404 ^d	<i>med-1(ok804); end-3(ok1448)</i>	42% (251)	23% (239)
E(30) / MS1763 ^{d,e}	<i>end-1(ok558) end-3(ok1448); Si[end-1(MED-)]</i>	28% (98)	< 5% (> 100)
E(0) / MS1762 ^{c,e}	<i>end-1(ok558) end-3(ok1448); Si[end-3(MED-)]</i>	0% (93)	0%
E(0) / MS1248 ^{c,f}	<i>end-1(ok558) end-3(ok1448)</i>	0% (190)	0%

^a Gut was scored by presence of any amount of birefringent gut granules.

^b Percentage of eggs laid that survive to adulthood.

^c Strain described in Maduro et al. (2015).

^d Strain described in Maduro et al. (2007).

^e These strains were maintained by an extrachromosomal array balancer carrying *end-3(+)* and a broadly-expressed *sur-5::dsRed* fluorescent reporter. Progeny embryos lacking the reporter were scored for the presence of gut.

^f Strain described in Owrighi et al. (2010).

laboratory propagation. We regularly obtained stocks of the original isolates of these strains from frozen storage, especially for work involving quantification of traits that tracked with the severity of the gutless phenotype. We note that while strain MS1763 did produce viable animals, the proportion of surviving adults was so low (< 5%) that we did not use this strain for most experiments. We performed detailed analyses on only a subset of the HGS strains as effects were generally similar across all strains in preliminary assays.

2.3. Microscopy, imaging and data analysis

Conventional epifluorescence and differential interference microscopy were performed on an Olympus BX-51 microscope, imaged through an LMscope adapter (Micro Tech Lab, Graz, Austria) and Canon Rebel T1i Digital Camera using software supplied with the camera. Confocal Microscopy was performed on a Zeiss 510 LSM at the UC Riverside Microscopy Core. To obtain staged embryos for the analyses in Fig. 4, gravid hermaphrodites were dissected with a 25-gauge needle and 4-cell stage embryos were collected and placed on an unseeded 6-cm agar plate and allowed to develop for 5 h in a 20 °C incubator. For microscopic observation, embryos were mounted as described (Bao and Murray, 2011). Images were combined, adjusted for color/contrast and cropped using FIJI (ImageJ) and Adobe Photoshop. To generate heat maps for Fig. 4, the summed Z-stack red channel (mCherry) images were converted to binary format with FIJI, where the red signal was converted to black, and the background to white. These images were compiled into a stack with the Images to Stack tool. Heat maps were generated with the heat map tool in FIJI on the newly built stacks. Plots were generated in ggplot2 in an R environment (<http://ggplot2.org>) or Microsoft Excel.

3. Results

3.1. An allelic series of strains affecting specification of (only) the gut

We have assembled a set of strains that specifically interfere with the MED-END regulatory chain in the early E lineage but which do not affect other tissues (Fig. 1C). Two of the strains never make gut, while control strains make gut 100% of the time. The remainder, which we call "Hypomorphic Gut Specification" (HGS) strains, exhibit a range of penetrance from 28% to 96% of embryos making gut (Table 1). Two of the HGS strains are chromosomal mutants, i.e. the single null mutant *end-3(ok1448)* and a double mutant of *med-1(ok804)* and *end-3(ok1448)* (Maduro et al., 2005a, 2007). The remaining strains consist of an *end-1(ok558) end-3(ok1448)* double null mutant background with single-copy transgenes of *end-1* and/or *end-3* with mutated MED-1,2 binding sites (Maduro et al., 2015). To facilitate reference to the individual strains, we will use the notation E(X) to indicate a strain in which E makes gut in X% of embryos, rounded to the nearest multiple of 5 (see Table 1). In this work we use these strains to determine how effects on E lineage development correlate with effects on gut specification and development.

3.2. The E lineage becomes stochastic in partial-specification strains

We first used the HGS strains to determine the relationship between the degree of partial specification and changes in the E lineage. To evaluate production of gut nuclei, we used an integrated, nuclear-localized *elt-2::GFP* reporter, *wIs84*. We counted 20.0 ± 0.5 SD *elt-2*-expressing nuclei in E(100) controls, consistent with expectation (Table 2; Fig. 2A, panel a, Fig. 2B). We then counted the number of *elt-2::GFP*-expressing cells in late embryos of HGS strains containing at least one such cell. All strains, even the mildly affected E(95) strain, exhibited a wide range in the number of gut nuclei produced, from as few as 1 to as many as 34 nuclei (Fig. 2B). The mean number of nuclei, which varied from 7.3 ± 5.3 for the severe E(30) strain to 19.7 ± 6.7 for

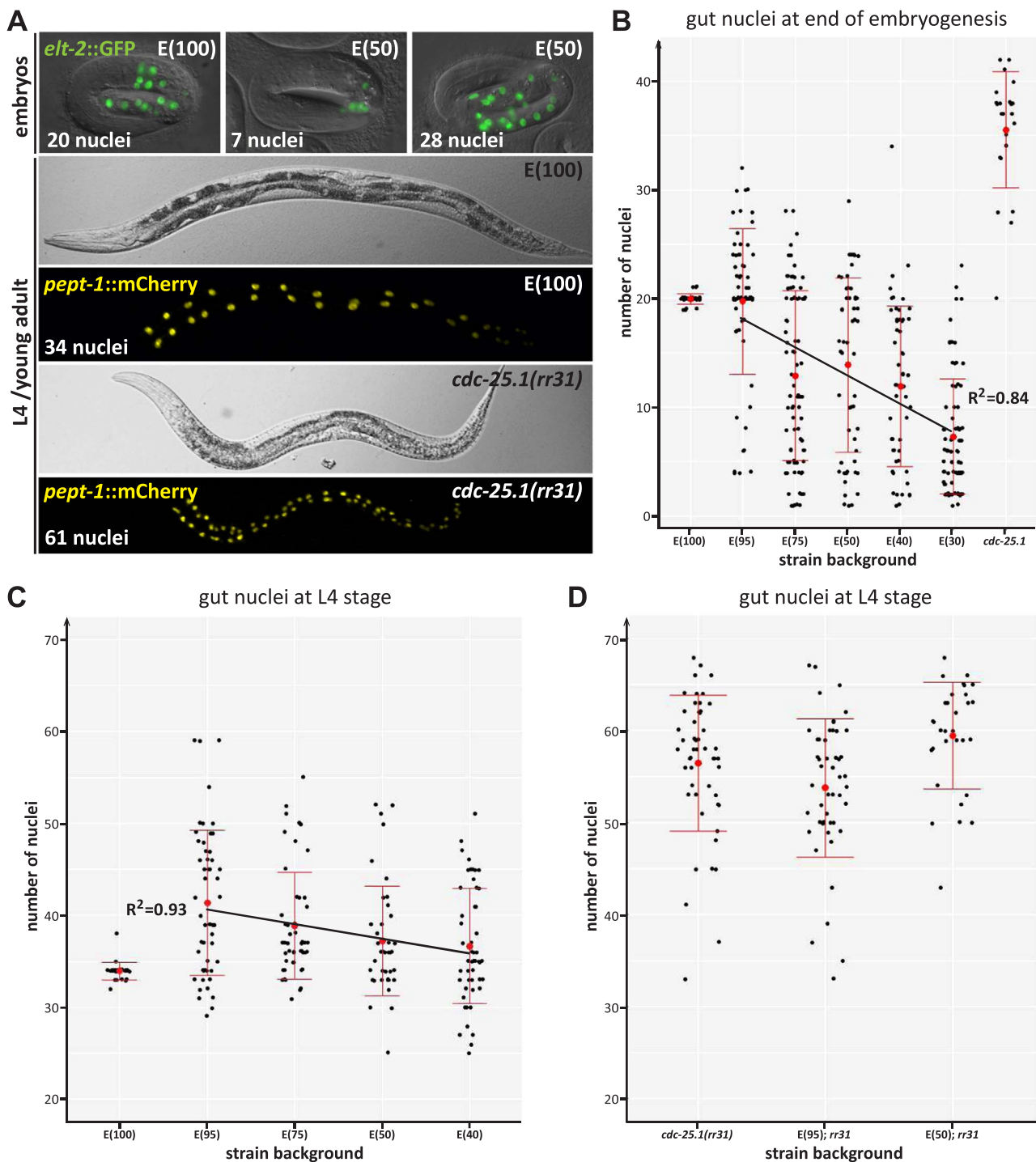


Fig. 2. Number of gut nuclei correlates with severity of specification defect in late-stage embryos, and less so in surviving L4 animals. (A) Examples of embryos (top row) and L4 animals (bottom two images). Gut nuclei were counted in living embryos homozygous for a nuclear-localized *elt-2::GFP* transcriptional reporter (*wIs84*), and in L4 animals with a single-copy nuclear-localized *pept-1::mCherry* reporter (*irSi24*), pseudocolored yellow. The embryo images are overlaid with a DIC image of the same embryo. An embryo is approximately 50 μm along its long axis, and the L4 intestines are approximately 750 μm long. Anterior is to the left. (B) Perturbation of specification causes aberrant numbers of gut nuclei to form, in a quantity proportional to the severity of the defect in specification. We note that the proportion of gut specification across the X-axis is not linear as shown. (C) Surviving L4 animals display a similar range of aberrant gut nuclei that may be only mildly correlated with severity of specification. All four of the specification strains had gut nucleus numbers significantly different from the control ($p < 0.004$, *t*-test). Compared with *end-3*, E(75) was not significantly different ($p=0.07$) while the other two strains were ($p < 0.005$). Pairwise differences among E(75), E(50) and E(40) were not significant ($0.06 < p < 0.2$). (D) The gain-of-function *cdc-25.1(rr31)* results in an increase in the number of gut nuclei that is not significantly enhanced by the E(95) or E(50) genetic backgrounds ($p=0.07$ and $p=0.05$, *t*-test). The E(95); *cdc-25.1* and E(50); *cdc-25.1* strains were significantly different from each other ($p=0.0003$).

the E(95) strain, correlated well with the percentage of embryos that make gut in the strain overall ($R^2 = 0.84$; note that the horizontal scale is not uniform). These results confirm across all the HGS strains that when an embryo contains gut-like cells, it does not mean that the gut is

normal; that is, gut specification is clearly not an "all-or-none" event, otherwise every embryo with gut should contain 20–22 nuclei expressing *elt-2::GFP*.

We were next interested in the variation in gut nucleus number in

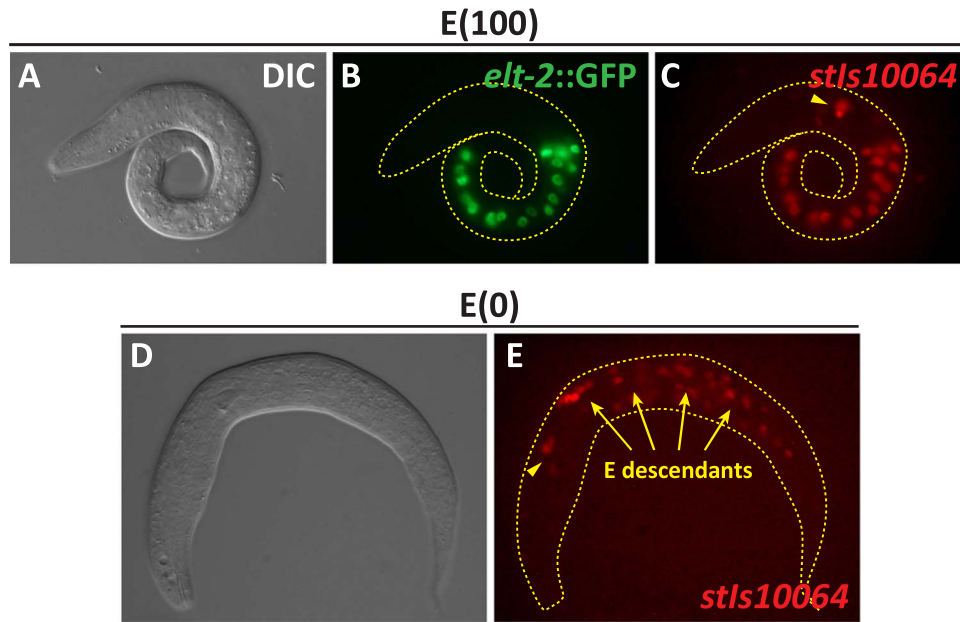


Fig. 3. A reporter that marks the E lineage. The *end-3::mCherry::H2B::let-858_3'UTR* reporter *stIs10064* (Murray et al., 2008) marks the descendants of E even when they do not make gut. (A–C) Control E(100) embryo. Panel (B) shows nuclei of intestinal cells. (C) The *stIs10064* reporter is expressed in the same nuclei as *elt-2::GFP*, plus a small number of nuclei in the head (arrowhead) that are likely to be neurons based on their location. (D, E) Arrested larva of strain E(0), *end-1(ok558) end-3(ok1448)*, with no intestinal cells (Owraghi et al., 2010). In such embryos, E adopts the fate of the C cell, and produces muscle and hypodermal cells (Maduro et al., 2005a; Owraghi et al., 2010). These ectopic C-like descendants are found in various positions throughout the larva (E). The ectopic expression in the head is also visible (arrowhead). Images are shown at the same scale. The larva in (D) is approximately 200 μ m long.

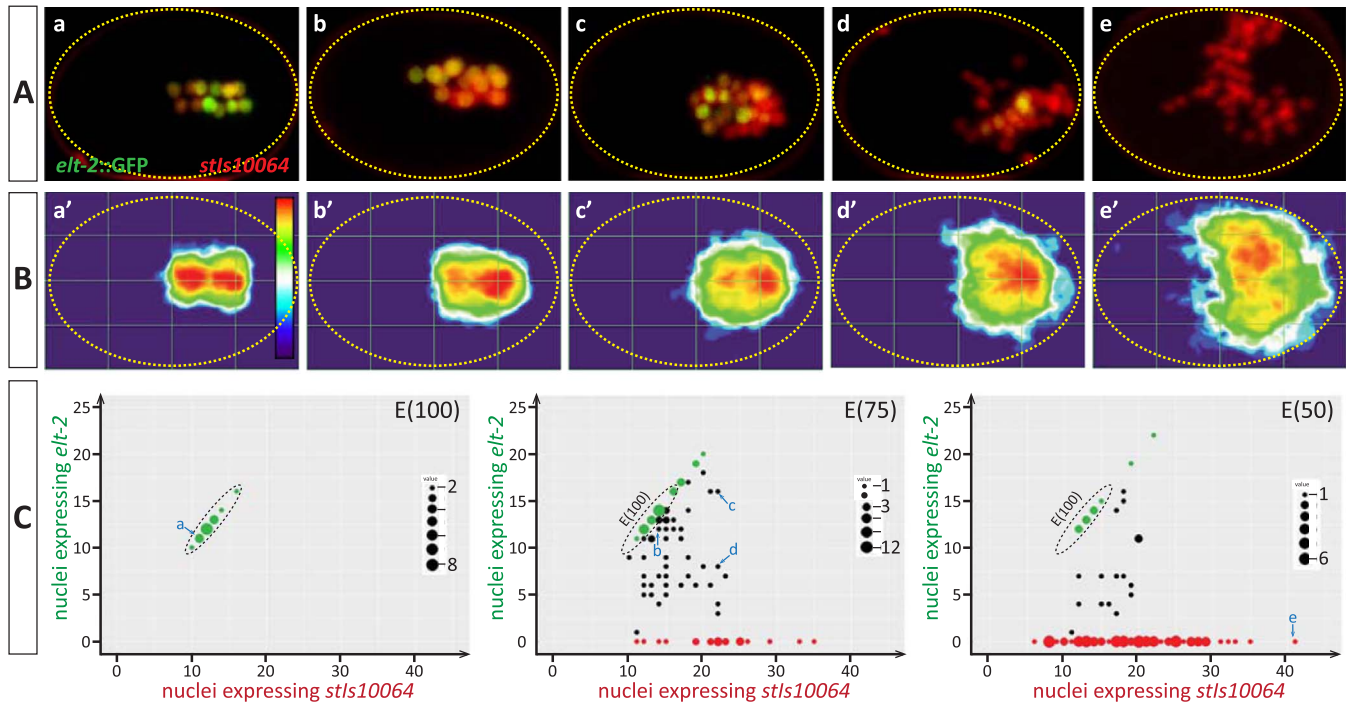


Fig. 4. Behavior of E lineage descendants that adopt gut or non-gut fates in HGS strains at 300–350 min past fertilization. (A) Representative maximum-value projections of confocal micrographs showing embryos produced by HGS strains, arbitrarily divided into five classes. *elt-2::GFP* expression (gut fate) is green and *stIs10064* expression (E lineage) is red. Panel a, wild type, in which all E descendants express *elt-2::GFP*. Panels b–e, progressively lower fractions of *elt-2::GFP*-expressing nuclei among E descendants, with no *elt-2* expression in panel e. (B) Heat maps showing location of E lineage descendants among multiple images with similar classes of percentage of *elt-2::GFP*-expressing nuclei, along a similar scale as the images in (A). The look-up table is shown in panel a'. (C) Two-dimensional plots of number of *elt-2::GFP*-expressing nuclei vs. number of *stIs10064*-expressing nuclei (E lineage descendants). Green dots indicate embryos in which all E descendants expressed *elt-2::GFP*; red dots indicate embryos in which none of the E descendants expressed *elt-2*; and black dots indicate embryos where a portion of the E descendants expressed *elt-2*. The dot sizes represent numbers of observations with scale shown at right within each plot. Lowercase letters (a–e) indicate the data points corresponding to embryos that appear in the row of images in (A). A dotted oval in the right two panels indicates the range of data obtained in the control. Embryos are shown with anterior to the left. A *C. elegans* embryo is approximately 50 μ m long.

Table 2
Number of gut nuclei among embryos making gut in strains affecting the E lineage.

Stage	Strain ^a						<i>cdc-25.1 (rr31)</i>	E(95); <i>rr31</i>	E(50); <i>rr31</i>
	E(100)	E(95)	E(75)	E(50)	E(40)	E(30)			
End of embryogenesis ^b	20.0 ± 0.5 (34)	19.7 ± 6.7 (63)	12.9 ± 7.8 (85)	13.9 ± 8.0 (54)	11.9 ± 7.4 (54)	7.3 ± 5.3 (79)	35.5 ± 5.4 (23)	nd ^c	nd
L4 ^d	33.9 ± 1.0 (29)	41.4 ± 7.9 (52)	38.9 ± 5.8 (50)	37.2 ± 6.0 (42)	36.6 ± 6.3 (51)	nd	56.5 ± 7.4 (51)	53.8 ± 7.5 (50)	59.5 ± 5.8 (31)

Numbers shown are mean ± SD with total number of embryos scored reported underneath.

^a See Table 1 for full strain genotypes.

^b Determined by scoring number of nuclei expressing *elt-2::GFP* reporter *wIs84*.

^c nd, not determined.

^d Determined by scoring number of nuclei expressing *pept-1::mCherry* reporter *irSi24*.

adults. The production of a small number of gut cells in the embryo is incompatible with survival past the first larval stage, as animals lacking a functional intestine arrest as embryos or L1 larvae (Fukushige et al., 1998; Owrighi et al., 2010). Whereas newly hatched larvae contain 20 intestinal nuclei, adults contain 34: During the L1 stage, 14 gut nuclei undergo a division without cytokinesis, bringing the total number of nuclei to 34, though the number can vary slightly (Sulston and Horvitz, 1977). Recent work suggests that animals can survive to adulthood with fewer than 20 gut cells. Loss of *cdc-25.2* function results in embryos that make only 16 gut nuclei, as the last four divisions in E development do not occur (Lee et al., 2016). The adults from such embryos retain 16 gut nuclei, as the postembryonic binucleations also become suppressed. Hence, depending on whether or not binucleations occur in HGS strains, we might expect to see fewer than 34 gut nuclei among surviving adults. To count adult intestinal nuclei, we used a single-copy transgene reporter, *irSi24*, which carries a nuclear-localized *pept-1::mCherry* fusion (Maduro et al., 2015). In the control we counted 33.9 ± 1.0 nuclei as expected (Table 2; Fig. 2A, panel d, and Fig. 2C). Among the HGS strains we tested, counts of gut nuclei varied from as few as 25 to as many as 59 (Fig. 2C). The mean numbers across HGS strains ranged from 36.6 ± 6.3 in E(40) to 41.4 ± 7.9 in E(95), and we found a similar correlation between the gut nucleus counts and HGS severity among the HGS strains ($R^2=0.93$). An increase in cell divisions might be due to either a partial transformation to an alternate fate, as the other fates acquired by E in specification backgrounds are C or MS, which make 47 and 80 cells, respectively (Maduro, 2015; Sulston et al., 1983).

The numbers of embryonic and adult gut nuclei allow us to infer the occurrence of postembryonic nuclear divisions in most (if not all) surviving HGS embryos. For each HGS strain, we sorted the numbers of gut nuclei from highest to lowest, then took the top fraction that correspond to the viability of the strains as reported in Table 1. This produces average numbers of embryonic gut nuclei that range from 20.7 ± 4.1 for E(40) to 22.4 ± 3.6 for E(95). Compared with the average numbers of gut nuclei at L4 of 36.6 ± 6.3 in E(40) to 41.4 ± 7.9 in E(95) reported above, we can infer that ~16 to 19 postembryonic nuclear divisions occur across surviving HGS embryos. This is higher than the wild-type number of 14, suggesting that some of the extra gut nuclei in HGS embryos also undergo a postembryonic division. There is evidence for such additional nuclear divisions in the *cdc-25.1(rr31)* strain, in which there are an average of 21 more nuclei between late embryos and L4s (Table 1).

The survival of L4 animals with fewer than 30 gut nuclei (Fig. 2C) can also be used to estimate the minimum number of embryonic gut nuclei that are compatible with survival past the larval stages in the HGS strains, by taking the lowest number of nuclei in the proportion of survivors. These are 17 for E(95), 15 for E(75), 19 for E(50) and 18 for E(40). These numbers are approximately consistent with prior results that 16 embryonic gut nuclei are compatible with survival (Lee et al., 2016), but in the case of the more strongly affected HGS strains, a

slightly higher number of gut nuclei may be required for viability.

Overall, these results confirm that among all HGS strains, the number of gut nuclei produced in embryos and adults correlates with the severity of the gut specification defect.

3.3. Production of extra gut cells in HGS strains does not synergize with *cdc-25.1(gf)*

Gain-of-function mutations in *cdc-25.1* result in extra cell divisions in the developing E lineage, resulting in excess gut nuclei in the embryo and adult without affecting gut specification and viability (Clucas et al., 2002; Kostic and Roy, 2002). Embryos from *cdc-25.1(rr31)* mothers contain an average of 38 ± 3 gut nuclei, and adults have 57 ± 4 (Kostic and Roy, 2002), which is greater than the number we observed in our HGS strains. We wished to determine whether HGS gut nucleus increases might synergize with *cdc-25.1* gain-of-function to produce animals with even more E descendants. Control *cdc-25.1(rr31)* embryos displayed an average of 35.5 ± 5.6 nuclei in embryos and 56.5 ± 7.4 as adults (Table 2; Fig. 2B,D), close to expectation (Kostic and Roy, 2002). In the E(95) background, *cdc-25.1(rr31)* adults had an average of 53.8 ± 7.5 nuclei, and in E(50), 59.5 ± 5.8 (Fig. 2D). Both are on the border of significance ($0.05 \leq p \leq 0.07$) when compared with *cdc-25.1(rr31)* alone, but have $p=0.0003$ when compared with each other (Student's *t*-test). Paradoxically, the individual E(95) and E(50) backgrounds exhibited different means (41.4 ± 7.9 for E(95) and 37.2 ± 6.0 for E(50), $p=0.005$) but in the opposite direction, i.e. E(50) had fewer gut nuclei on average than E(95) (Fig. 2C). We make the conservative conclusion that HGS backgrounds combined with *cdc-25.1(rr31)* do not cause a further increase in adult gut nucleus numbers over what occurs in *cdc-25.1(rr31)* alone. This suggests that the mechanism by which HGS backgrounds cause an increase in cell division is either through CDC-25.1, or there may be an intrinsic limit to the number of gut descendants that can be made from the E founder cell (or a combination of both).

3.4. A marker that identifies E lineage descendants independently of their fate

We previously proposed that HGS strains experience hyperplasia within the E lineage, although the proportion of E descendants that adopt a gut fate can vary, resulting in significantly fewer than 20 gut nuclei in some embryos (Maduro, 2015). To directly test this hypothesis, we attempted to follow the E lineage over time in HGS embryos carrying the *wIs84 elt-2::GFP* reporter by introducing ubiquitously-expressed nuclear-localized mCherry reporters (Murray et al., 2008). In control embryos, we observed onset of *elt-2::GFP* in the 8E stage as expected. By following a small number of embryos by 4D time lapse in the E(50) background, we identified one in which the posterior four of the 8E cells activated *elt-2::GFP*, validating the notion that it is possible for part of the E lineage to acquire *elt-2::GFP* expression. However, we

were unable to reliably follow all of the descendants of E in time lapse recordings due to the increased number of such cells and their novel positions as described below.

An alternative approach to following E descendants in time lapse would be to use a reporter that was specific to the E lineage, but independent of the fate adopted by its descendants. Embryos could then be observed at any stage, even when the location of the descendants, and cell division pattern, are not the same as in the wild type. We hypothesized that a transgene reporter for *end-3* should be activated normally in the early E lineage in all HGS backgrounds, and as long as the reporter did not provide functional END-3 protein, it would also not interfere with specification. However, our existing *end-3* transgenes are expressed only from the 2E through 8E stages (Maduro et al., 2005a). Others have described an *end-3::mCherry* transgene, *stIs10064*, that shows expression long past the 8E stage (Murray et al., 2008). We confirmed persistent expression of *stIs10064* in the E lineage at multiple stages (Fig. 3A–C and data not shown). To confirm that *stIs10064* marks E descendants even when gut is not made, we crossed this reporter into the *end-1(ok558) end-3(ok1448)* double mutant background (Owraghi et al., 2010). Expression was detectable even when E failed to be specified for gut (Fig. 3D,E). We note that past the two-fold stage, additional non-intestinal expression occurs from *stIs10064* in 2–4 small cells near the nerve ring, suggesting these are neurons (Fig. 3C,E).

3.5. Gut misspecification causes extra divisions and stochastic acquisition of gut fate within the E lineage

We crossed *stIs10064* and *elt-2::GFP* into the HGS strains to simultaneously mark all E descendants and the subset of these that acquires a gut fate, and chose the E(75) and E(50) backgrounds for further study. We obtained image stacks by confocal microscopy at approximately 300–350 min after fertilization, representing the 8E–16E stage of gut development, a time when the embryo and gut primordium have not yet undergone extensive elongation (Asan et al., 2016; Sulston et al., 1983). We imaged embryos for GFP and mCherry and summarized the results in Table 3 and Fig. 4, sorting the images into categories by the proportion of E descendants adopting a gut fate, generating a heat map to localize the E descendants across the various categories, and plotting *elt-2::GFP* nuclei vs. *stIs10064* nuclei. As expected, control embryos showed colocalization of *elt-2::GFP* and *stIs10064* in the middle-posterior of the embryo, and 10–16 nuclei consistent with the time window of observation (Fig. 4A, panel a; Fig. 4B, panel a'; Fig. 4C, left plot). Among both E(75) and E(50)

Table 3

Summary of E lineage vs. *elt-2::GFP* expression data at 300–350 min past fertilization.

	Strain		
	E(100) (n=22)	E(75) (n=100)	E(50) (n=100)
Average # of E descendants	12.4 ± 1.6 ^a	16.7 ± 4.8	18.4 ± 6.7
Average # of <i>elt-2::GFP</i> -expressing nuclei	12.4 ± 1.6	9.1 ± 6.0	2.6 ± 5.2
% of embryos in which all E descendants expressed <i>elt-2::GFP</i>	100%	33%	9%
% of embryos in which some (but not all) E descendants expressed <i>elt-2::GFP</i>	0%	46%	16%
% of embryos with no <i>elt-2::GFP</i>	0%	21%	75%

^a SD.

backgrounds, we observed a spectrum of embryos that showed from as few as a single *elt-2::GFP*-expressing cell to as many as 24 (Fig. 4A, panels b–e; Fig. 4C, center and right-most plots). Across both HGS strains, the number of E descendants, marked by *stIs10064*, ranged from 6 to 41, and the number of *elt-2::GFP* nuclei ranged from 0 to 24. The control embryos had an average of 12.4 ± 1.6 E descendants, all of which expressed *elt-2::GFP*. The milder HGS strain E(75) showed an average of 16.7 ± 4.8 E descendants, while the more strongly affected E(50) strain showed an average of 18.4 ± 6.7. When fewer E descendants exhibit *elt-2* reporter expression in an embryo, the E descendants tend to migrate to positions away from the normal location of the gut primordium in the middle posterior (Fig. 4A,B).

The results reinforce the notion that the fate of E in partially compromised strains is not consistent with a "wholesale" transformation to an alternate fate (Maduro et al., 2015; Owraghi et al., 2010). We can make the following conclusions about the HGS strains: First, the number of E descendants made is generally at least as many as in the controls. Second, specification occurs stochastically among the E descendants, as opposed to E itself, as 46% of the E(75) embryos, and 16% of the E(50) embryos, exhibited expression of *elt-2::GFP* in a variable subset of E descendants. Third, the greater the probability that a strain fails to specify any gut, the greater the number of E descendants are produced, of which fewer adopt a gut fate, and the farther away from the middle-posterior of the embryo these migrate. The correlation between severity of the specification defect and the effect on the E lineage suggests that gut cells in HGS embryos result from stochastic acquisition of gut fate among the descendants of E.

3.6. HGS strains delay activation of *ELT-2*, but final levels appear normal

END-1 and END-3, with contribution from ELT-7, ultimately activate *elt-2* to maintain differentiation of intestinal cells (Du et al., 2016; Fukushige et al., 1998; Sommermann et al., 2010; Wiesenfahrt et al., 2015). Expression of *elt-2* is then maintained by positive autoregulation (Fukushige et al., 1999). The HGS strains exhibit stochastic specification of gut fate among descendants of E, suggesting that activation of *elt-2* becomes delayed until later time points in the lineage, and that its activation is stochastic. Others have observed delayed activation of a transcriptional *elt-2* reporter in the *end-3* mutant background (Boeck et al., 2011). As the more strongly affected HGS strains produce fewer gut cells overall, it is reasonable to hypothesize that activation of *elt-2* in these strains becomes further delayed.

To evaluate onset of *elt-2* activation, we used the *wIs84* reporter. We examined several HGS backgrounds and observed embryos in real time under fluorescence microscopy to detect onset of expression. As predicted, among HGS embryos activating *wIs84*, onset was variable, with delayed onset correlating with severity of the specification defect across the strains (Fig. 5A). Whereas control embryos experienced *elt-2::GFP* onset an average of 2.9 ± 0.6 h after four-cell stage, the HGS strains were delayed by 0.6 – 1.7 h with standard deviations ranging from 0.5 to 1.0 ($p < 10^{-4}$, Welch's T-test). All embryos that activated *elt-2* retained expression until the end of embryogenesis, consistent with *elt-2* onset marking the commitment to a gut fate.

The positive autoregulation of *elt-2* suggests that even when initiation of expression is delayed, final expression levels should normalize to levels seen in the wild type (Fukushige et al., 1999). We therefore examined embryos for their steady-state levels of *elt-2* expression. The transcriptional reporter in *wIs84*, which we used above, may not accurately portray steady-state levels of expression of ELT-2, as it lacks most of the ELT-2 coding region (Fukushige et al., 1998). Instead, we used a different reporter, *galS290*, a chromosomal insertion of a fosmid clone carrying the *elt-2* genomic region and surrounding genes with an in-frame GFP insertion into the coding region of ELT-2 (Mann et al., 2016; Sarov et al., 2006). We crossed *galS290* into the E(95) and E(40) backgrounds and obtained fluores-

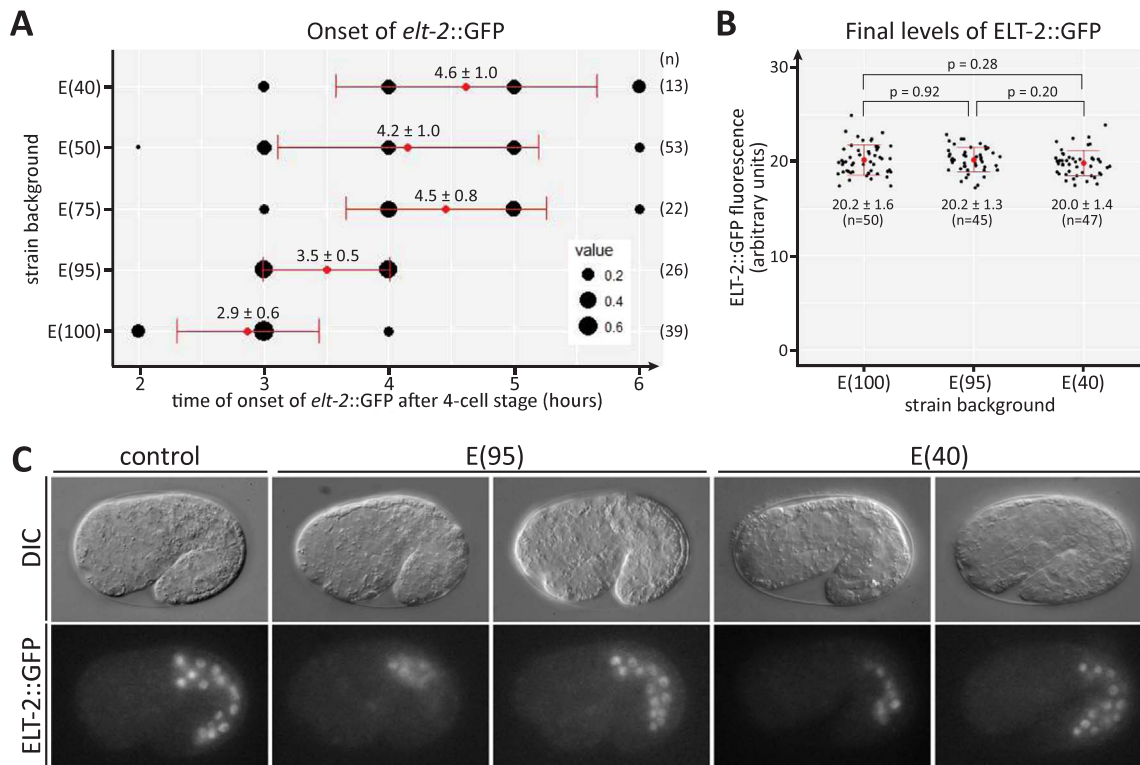


Fig. 5. ELT-2 activation is delayed but achieves normal levels in HGS strains. (A) Time of onset of *elt-2::GFP* transcriptional reporter *wIs84* in various backgrounds. Embryos were observed at 23–25 °C starting at the 4-cell stage (0 h) and onset of GFP expression determined by checking fluorescence every 60 min. Dot size corresponds to the proportion of embryos exhibiting onset at that time point after four-cell stage. Means ± SD are reported and indicated in red and the number of GFP(+) embryos scored is shown to the right of the graph. Embryos that did not activate the reporter were not included in the plot. (B) Expression levels of the *gals290* translational ELT-2::GFP reporter. Fluorescence of individual nuclei was measured using ImageJ on digital images at 1.5-fold stage (identified by morphology) taken using identical settings across all embryos. Nuclei were chosen for analysis only if they were in focus (sharp outer edge and nucleolus). (C) Representative single focal plane images of 1.5-fold stage embryos expressing *gals290*. In the E(95) and E(40) examples, embryos are shown that contained too few and an approximately normal number of nuclei. For these panels, fluorescence images were taken at identical settings across all embryos, made monochrome and adjusted for contrast using the same settings. Embryos are approximately 50 μm long.

cence images of 1.5-fold embryos that we analyzed using ImageJ. Among control, E(95) and E(40) embryos, levels were indistinguishable (Fig. 5B; $p \geq 0.2$ across all pairwise comparisons, Welch's *t*-test). The expression levels did not change with the number of *elt-2*-expressing cells present (Fig. 5C). Acquisition of relatively normal *elt-2* reporter expression has been observed in the E(95) background in a prior work (Wiesenfahrt et al., 2015).

Our results strongly suggest that a delay in the specification of gut fate is the basis for the stochastic activation of *elt-2* among the descendants of E. Despite a delay in expression onset, however, cells that activate *elt-2* ultimately achieve relatively normal levels of ELT-2 protein. The results show that the E cell cycle is exquisitely sensitive to timely activation of specification, as even the most mildly affected strain, E(95), demonstrates high variability in the number of cells produced by E. This effect is common to all of the HGS strains. The ultimate specification of gut fate, however, can be delayed at the expense of a reduction in the proportion of E descendants that activate *elt-2*. Forced early expression of ELT-2, even in the absence of *end-1* and *end-3*, can generate an apparently normal intestine (Wiesenfahrt et al., 2015), further consistent with delay of ELT-2 being the major cause of the defects we observe in the HGS backgrounds. However, in the HGS strains E(75) and E(40), we previously reported that adults demonstrate abnormal accumulation of lipids (Maduro et al., 2015), suggesting that delayed specification has other effects on gut differentiation that are not compensated by ELT-2 in later stages (see Discussion).

3.7. The gut primordium accommodates supernumerary cells in two ways

The varied numbers of gut nuclei made in HGS embryos fall into

two broad classes. In the first class, too few nuclei are present to allow formation of a normal gut. This is entirely consistent with how the *C. elegans* embryo develops, as neither compensatory proliferation (increase in cell number) nor compensatory hypertrophy (increase in cell size) have been reported to occur in the intestine, as occur in other animals in response to injury, for example (Haynie and Bryant, 1977; Ryoo and Bergmann, 2012; Tamori and Deng, 2014). Ablation of part of the gut primordium shows that portions of the gut can develop in a mosaic fashion, although the degree of morphogenesis strongly depends on which parts of the gut remain (Leung et al., 1999). As described earlier, our HGS strains suggested that partial guts with fewer than ~15 cells do not support survival past the L1 stage.

In the second class of HGS embryo, there are approximately as many nuclei as in the wild type, and often an excess (Fig. 2B). The survival of such embryos implies that organogenesis of the *C. elegans* intestine is able to compensate, or regulate, with respect to the number of nuclei in the gut. The apparent normal development of *cdc-25.1(rr31)* mutants, which have an average of ~75% more gut nuclei at the end of embryogenesis, suggests this is the case (Kostic and Roy, 2002). As our HGS strains affect both the cell lineage and cell fate, we wished to examine whether the extra embryonic nuclei that we observe in the HGS strains, and those in *cdc-25.1(rr31)* embryos, correspond to extra cells, and if so, how the extra cells assemble into the gut, apparently oblivious to the extra nuclei present.

To visualize the gut primordium in living embryos, we obtained marker *zuls70* that carries an *end-1::GFP::CAAX* membrane-targeted GFP fusion that labels the cytoplasmic face of the membrane in the developing gut (Asan et al., 2016; Rasmussen et al., 2013; Wehman et al., 2011). To simultaneously visualize gut nuclei, we constructed an *elt-2::mCherry::H2B* reporter. We used control, E(95) and *cdc-*

25.1(*rr31*) backgrounds to evaluate gut development. The E(95) background was chosen as it generates the widest array of gut nucleus numbers among the HGS strains and is generally healthy (see Fig. 2B).

We first examined embryos in all three backgrounds and examined whether nuclei that were clearly expressing *elt-2::mCherry* were individually surrounded by a membrane. Using *zuIs70*, we confirmed that 136 nuclei of the control, 155 of the E(95) background, and 142 of the *cdc-25.1(rr31)* background are surrounded by a membrane over 12–14 embryos per strain. Conversely, we found no examples of cells with more than one *elt-2::mCherry* nucleus. We conclude that gut nuclei in HGS and *cdc-25.1(rr31)* embryos correspond to individual mononucleate cells, even if the number of cells is in excess.

We next examined the gross effects of supernumerary gut cells on appearance of the primordium during morphogenesis. A recent work describing the detailed development of the gut, using the same *zuIs70* marker, served as reference (Asan et al., 2016). In the wild type, the 20-cell primordium is visible as nine groups of cells that form intestinal 'rings' called int1 through int9 (Asan et al., 2016). The anterior-most four cells form int1, while the remaining 8 pairs of cells form int2 through int9. Prior observations suggest that extra cells in the gut can be accommodated in one of two ways. The first is that the intestinal rings can be made of more than two cells. This is supported by the observations that the anterior-most ring int1 already consists of four cells and that some mutant backgrounds suggest rings with 3 cells are possible (Asan et al., 2016). The second way that extra cells may be incorporated into the gut is through the formation of extra intestinal rings. This is suggested by the way that normal formation of the last ring, int9, occurs late in gut development when a substantial portion of the primordium is already present (Asan et al., 2016).

We examined embryos using both *zuIs70* and *elt-2::mCherry* at the beginning of embryo elongation, and again at mid-elongation, around the 1.5-fold stage. During this time, cells within the developing intestine undergo intercalations and rotations of the rings around the future lumen, while the intestine also becomes longer, and resolves into the future int rings (Asan et al., 2016). Sample images are shown in Fig. 6. We were able to resolve cells in control gut primordia as expected (Fig. 6A–D, M–P). In particular, we observed 9 rings ($n=57$ embryos) with a highly stereotyped cell arrangement similar to that described in Asan et al. (2016). In the E(95) background, we frequently observed cell arrangements and contacts that differed from wild type (Fig. 6E–H). At 1.5-fold elongation, guts exhibited both supernumerary rings and apparent extra cells in some rings (Fig. 6Q–T). Of 43 E(95) embryos with excess gut nuclei, 53% exhibited extra intestinal rings, 30% had excess cells per ring (but a normal number of 9 rings), and 16% showed both extra rings and extra cells per ring.

To confirm that these changes were the result of cell cycle alterations and not possible changes in cell fate, we examined the gut primordia in the *cdc-25.1(rr31)* background. At the start of elongation, the primordium contained an excess of cells that maintained cohesion but nonetheless assembled in the correct overall location in the embryo (Fig. 6I–L). The appearance of the cells was strikingly more abnormal in appearance than in E(95), likely due to the higher number of extra cells in this background. Despite this appearance, at elongation the gut primordia in *cdc-25.1(rr31)* resolved into an elongated shape (Fig. 6U–X). There were clear examples of both extra rings (four extra in the embryo shown in Fig. 6W–X) and extra cells (marked by red shading) in positions consistent with future incorporation into rings with more than two cells. Of 69 embryos, 33% exhibited extra rings, 23% had extra cells per ring, and 43% showed both extra rings and extra cells per ring. Hence, for both E(95) and *cdc-25.1(rr31)*, extra gut cells are accommodated by both the presence of extra intestinal rings, and extra cells per ring.

It is possible that in the E(95) *cdc-25(gf)* backgrounds, extra cells become excluded from the gut in later stages. However, in our scoring of intestinal nuclei in young adults (Fig. 2), we did not observe *elt-2-* or *pept-1*-expressing nuclei that were outside of the gut, suggesting that

all E descendants that adopt a gut fate persist and are incorporated into the intestine, and that exclusions of such cells from the intestine are rare. Furthermore, the increase in numbers of gut nuclei in young adults compared with embryos (Fig. 2B,D) was consistent with survival of embryonic gut cells to adulthood.

4. Discussion

In this work we have advanced our prior studies of gut specification by focusing on the collective behavior of E descendants in backgrounds that partially compromise gut specification (Maduro et al., 2005a, 2015, 2007). The relative simplicity of the *C. elegans* gut, in its specification, development and anatomy, contrasts with that of other systems. In *Drosophila*, the embryonic midgut arises from cells that invaginate from the posterior and anterior of the embryo (Reuter, 1994). The adult gut is generated during metamorphosis, contains stem cells, and is capable of regeneration (Lemaitre and Miguel-Aliaga, 2013). Loss of the *Drosophila* embryonic midgut specification factors *srp* or *dGATAE* results in embryonic lethality (Okumura et al., 2005; Rehorn et al., 1996). In the far more complex development of vertebrates, the liver, the first endodermal organ to be specified, has distinct functions in the embryo and adult (Zaret, 2016). Loss of the endoderm specification genes *GATA4/6* or *HNF-3b/FoxA2* is also lethal (Ang and Rossant, 1994; Holtzinger and Evans, 2005). Hence, the *C. elegans* intestine represents a more tractable system in which to study organogenesis from embryo to adult, and in which mutations in gut specification genes can be compatible with development.

Our results show that a loss of robustness in gut specification differentially affects cell division pattern (Fig. 2), commitment to endoderm fate (Figs. 4, 5), and gut morphogenesis (Fig. 6), in a highly stochastic manner. The results show that wild-type cell divisions and acquisition of gut fate require the timely and robust expression of *END-1* and *END-3*, an idea raised in our prior studies (Maduro et al., 2015). When activation of the *ends* is partially abrogated, commitment to gut differentiation becomes delayed and stochastic within the descendants of E. Our results are similar to those observed with interference of *Wnt/β-catenin* asymmetry, which directly affects activation of *end-1* and *end-3* (Robertson et al., 2014; Shetty et al., 2005), and a partial transformation of E fate observed some *pop-1; end-1,3* embryos (Owraghi et al., 2010). In these cases embryos did not complete morphogenesis, hence it was not possible to isolate effects on development to only the E lineage, or to follow the gut to adulthood, as we have done here. Nonetheless, it is apparent that perturbation of zygotic specification can reveal more nuanced effects on organogenesis. In our HGS strains, even mild compromise of specification resulted in supernumerary descendants of E, showing that the correct pattern of cell divisions is exquisitely sensitive to partially compromised specification, even when the majority of embryos make a functional gut.

The results also show that there is a proportional response to the delay in commitment to gut fate, as revealed by initiation of expression of a translational *ELT-2* reporter. The stronger the specification defect, the later the acquisition of gut fate, the lower the proportion of cells that do so, and the more the descendants migrate away from the normal location of the gut primordium. These correlations are consistent with a probabilistic model of *elt-2* transcription initiation, resulting from stochastic accumulation of *END-1* and *END-3* in the various HGS strains. This model extends the binary fate choice model proposed by Raj et al. (2010) that explains why ~20% of progeny embryos from a *skn-1* mutant mother make gut. In their model, gut specification depends on a threshold reached by stochastic levels of *end* mRNA (Raj et al., 2010). Our results show that this binary choice can occur among the descendants of E when activation of *end-1* and/or *end-3* are perturbed zygotically. Studies to model the effects of endoderm gene network perturbations are in progress (S. Rifkin, personal communication).

We observed variable commitment to gut fate among the descen-

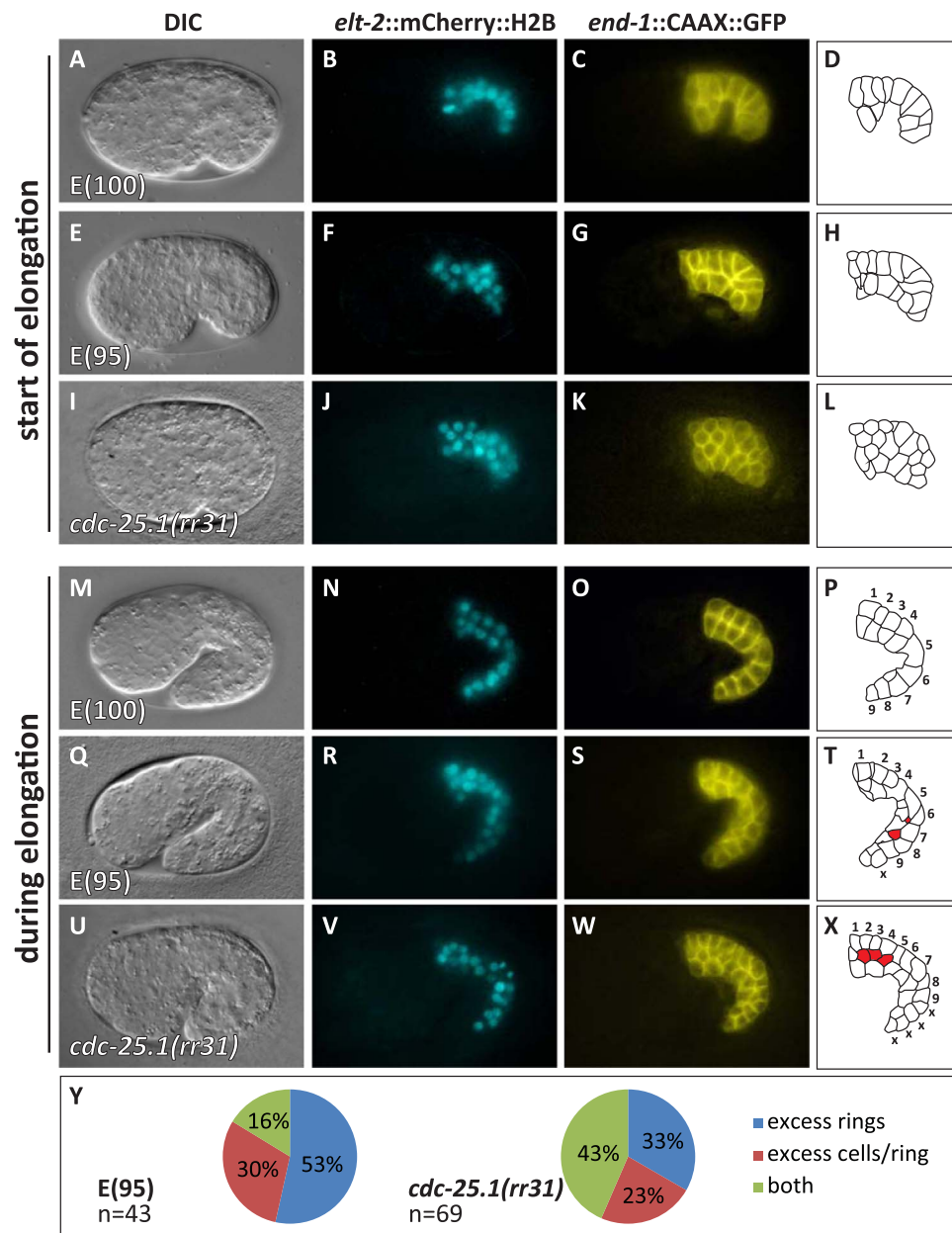


Fig. 6. Developing gut primordia appear to accommodate extra gut cells by adding additional cells per intestinal ring and adding extra rings. (A–L), start of embryo elongation. Gut primordia with extra nuclei adopt unusual positions (panels H, L) compared with control (D). (M–X) During elongation, patterns of intestinal ring formation show that extra cells adopt positions consistent with rings with extra cells (red cells in panels T and X) or form extra intestinal rings (letter 'x' in T and X). The control E(100) strain was made by crossing an *irSil2* integrated *end-1,3(+)* rescue transgene into the E(95); *zUs70* background. The *elt-2::mCherry::H2B* and *end-1::CAAX::GFP* expression were pseudocolored cyan and yellow. (Y) Pie charts showing proportion of embryos exhibiting excess rings, excess cells per ring, or both.

dants of E in HGS strains. If not gut cells, what do these non-gut E descendants become? The apparent migration of many of these non-gut E descendants away from the interior of the embryo suggests that these adopt adhesion and migratory behaviors of other cell types (Figs. 3 and 4A). When complete transformations in E fate occur as a result of complete loss of *end-1* and *end-3*, E adopts the fate of the C cell, which normally produces hypodermis and muscle (Hunter and Kenyon, 1996; Maduro et al., 2005a; Zhu et al., 1997). Among all HGS strains we observe at least some embryos that completely lack gut and which resemble *end-1,3(null)* double mutants, suggesting that when some E descendants fail to adopt a gut fate, they adopt fates consistent with a partial E-to-C transformation in fate. Consistent with this, the E descendants of embryos lacking gut generally adopt posterior positions in the embryo (Fig. 4), which is consistent with where muscle and hypodermal descendants of C are found (Sulston et al., 1983). We have

observed expression of the muscle-specific *hlh-1::GFP* reporter in non-gut E descendants, and hypodermis-like cavities are sometimes seen in HGS embryos with partial guts, consistent with acquisition of C-like fates (Chen et al., 1994) (data not shown). We note that it is possible that the presence of these non-gut cells interferes with morphogenesis, contributing to the lethality that is observed among HGS embryos.

Our results imply additional functions in the early endoderm specification network that regulate organ-level properties of the gut. These arise from the observation that steady-state levels of the differentiation factor ELT-2 appear to be normal in surviving HGS embryos and adults irrespective of the number of nuclei. We can infer that cell cycle changes in the E cell lineage that produce extra E descendants are determined before, and are subsequently not affected by, expression of ELT-2. This is evident in the E(95) strain in which onset of ELT-2 is delayed by an average of only 35 min, yet this strain

produces a wide range of gut cell numbers among embryos. Aside from the cell lineage, there are likely to be changes in gut function in HGS strains. We previously observed that surviving E(75) and E(30) animals exhibit various pleiotropic effects, including a delay in postembryonic development, that are similar to those seen with dietary restriction (Maduro et al., 2015; Palgunow et al., 2012). We have not observed such defects in the *cdc-25.1(rr31)* background, suggesting that supernumerary cells are not likely to be the cause of these defects (our unpublished results). There may therefore be additional target genes within the embryonic endoderm network that establish a normal pattern of cell divisions and metabolism; alternatively, delayed activation of ELT-2 may miss a time window in which normal patterns of ELT-2 target gene expression must be established.

Additional subtle defects likely exist within the intestine in surviving HGS adults as a result of changes in the cell lineage. Asan et al. (2016) observed that the lumen may contain abrupt changes in its orientation along the anterior-posterior axis if pairs of intestinal ring cell rotations fail to occur properly. As the embryonic ring rotations in normal embryos involve complex cell-cell interactions, it is likely that subtle defects in gut morphogenesis may occur in embryos with an excess of gut cells, especially as it appears that the arrangement of cells in such embryos is aberrant (Fig. 6). Future studies with additional markers will allow an assessment of more subtle aspects of gut morphology in HGS adults.

As part of our study of the HGS strains, we used a novel transgene, *stIs10064*, to mark the E lineage irrespective of the fates adopted by the E descendants (Fig. 4). We were interested in why *stIs10064* continues to be expressed until the end of embryogenesis, when endogenous *end-3* and our prior *end-3* reporters are restricted to the early E lineage (Maduro et al., 2005a). This does not appear to be due to additional regulatory input of *stIs10064*, as E lineage expression of *stIs10064* is abolished in *med-1(ok804); med-2(cxTi9744)* double mutant embryos (not shown), similar to the *end-3::GFP* reporter *wIs137* (Maduro et al., 2015). Rather, a comparison of known *end* reporters suggested to us that the transgene mRNA in *stIs10064* is stabilized by the presence of the 3'UTR of *let-858* in the reporter. Indeed, all of the reporters in Murray et al. (2008) exhibit persistence of embryonic expression after initial onset, likely for the same reason. Hence, this method of labeling descendants in cell specification mutants could theoretically be applied to any lineage.

We have also shown that even though HGS embryos produce widely varying numbers of gut cells, as long as there are a sufficient number of them, the developing gut can accommodate these during morphogenesis. Our evidence suggests that from the E8 to E16 time period, the developing intestine incorporates extra cells into the gut both by forming rings with extra cells and by forming extra rings. This ability is consistent with the > 80% viability of E(95) and the reported ~100% viability of *cdc-25.1(rr31)* (Kostic and Roy, 2002), both of which exhibit increased and variable numbers of gut cells (Fig. 2B). These results suggest that the mechanisms that drive morphogenesis of the *C. elegans* intestine are robust to changes in the number of descendants of E when there are sufficient cells to make a gut, and even when there are almost twice as many cells. This means that the reproducible cell behaviors that occur during intestine morphogenesis among wild-type animals likely result from the highly reproducible cell division patterns from animal to animal.

Our results are consistent with the notion that evolution of specification gene networks in *C. elegans* is biased to assuring the robustness of the earliest steps. Indeed, the early gut specification network contains multiple, parallel maternal inputs, but at the level of differentiation, ELT-2 is the principal factor (with minor input from ELT-7) that maintains gut fate (Fig. 1C) (Maduro et al., 2015; McGhee et al., 2009; Sommermann et al., 2010). Enforcement of timely gut progenitor specification also assures the generation of sufficient numbers of cells to form the intestine, as our stronger HGS strains exhibited fewer gut cells and reduced viability overall (Fig. 2B, Table 1).

The ability of the *C. elegans* gut to overcome drastic changes in the cell lineage may reflect an ancestral mode of organogenesis held over from species with more variable cell divisions. Over time, fine-tuning of the cell lineage may have favored a number of 20 cells because this is sufficient to make a functioning intestine while conserving the energy that would have been required for additional cell divisions. The HGS and *cdc-25.1(rr31)* strains, therefore, form a collection of strains in which to study organ-level mechanisms of morphogenesis that are robust to variability in the cell lineage.

Acknowledgments

We thank Christian Frøkjær-Jensen for bringing the *oxTi389* insertion to our attention, James Priess (Fred Hutchinson Cancer Center, Seattle, WA) for sending us strains, and an anonymous reviewer for helpful comments to improve the manuscript. Some strains were provided by the *Caenorhabditis* Genetics Center (CGC), which is funded by the NIH Office of Research Infrastructure Programs (P40 OD010440). This work was funded by NSF Grant IOS#1258054 to M.M.

References

- Ang, S.L., Rossant, J., 1994. HNF-3 beta is essential for node and notochord formation in mouse development. *Cell* 78, 561–574.
- Arribere, J.A., Bell, R.T., Fu, B.X., Artiles, K.L., Hartman, P.S., Fire, A.Z., 2014. Efficient marker-free recovery of custom genetic modifications with CRISPR/Cas9 in *Caenorhabditis elegans*. *Genetics* 198, 837–846.
- Asan, A., Raiders, S.A., Priess, J.R., 2016. Morphogenesis of the *C. elegans* intestine involves axon guidance genes. *PLoS Genet.* 12, e1005950.
- Bao, Z., Murray, J.I., 2011. Mounting *Caenorhabditis elegans* embryos for live imaging of embryogenesis. *Cold Spring Harb. Protoc.*, 2011.
- Blake, W.J., M., K.A., Cantor, C.R., Collins, J.J., 2003. Noise in eukaryotic gene expression. *Nature* 422, 633–637.
- Boeck, M.E., Boyle, T., Bao, Z., Murray, J., Mericle, B., Waterston, R., 2011. Specific roles for the GATA transcription factors *end-1* and *end-3* during *C. elegans* E-lineage development. *Dev. Biol.* 358, 345–355.
- Bowerman, B., Eaton, B.A., Priess, J.R., 1992. *skn-1*, a maternally expressed gene required to specify the fate of ventral blastomeres in the early *C. elegans* embryo. *Cell* 68, 1061–1075.
- Chen, L., Krause, M., Sepanski, M., Fire, A., 1994. The *Caenorhabditis elegans* MYOD homologue HLH-1 is essential for proper muscle function and complete morphogenesis. *Development* 120, 1631–1641.
- Clucas, C., Cabello, J., Bussing, I., Schnabel, R., Johnstone, I.L., 2002. Oncogenic potential of a *C. elegans* *cdc25* gene is demonstrated by a gain-of-function allele. *EMBO J.* 21, 665–674.
- Colman-Lerner, A., Gordon, A., Serra, E., Chin, T., Resnekov, O., Endy, D., Pesce, C.G., Brent, R., 2005. Regulated cell-to-cell variation in a cell-fate decision system. *Nature* 437, 699–706.
- Davidson, E.H., 2010. Emerging properties of animal gene regulatory networks. *Nature* 468, 911–920.
- Du, L., Tracy, S., Rifkin, S.A., 2016. Mutagenesis of GATA motifs controlling the endoderm regulator *elt-2* reveals distinct dominant and secondary cis-regulatory elements. *Dev. Biol.* 412, 160–170.
- Fukushige, T., Hawkins, M.G., McGhee, J.D., 1998. The GATA-factor *elt-2* is essential for formation of the *Caenorhabditis elegans* intestine. *Dev. Biol.* 198, 286–302.
- Fukushige, T., Hendzel, M.J., Bazett-Jones, D.P., McGhee, J.D., 1999. Direct visualization of the *elt-2* gut-specific GATA factor binding to a target promoter inside the living *Caenorhabditis elegans* embryo. *Proc. Natl. Acad. Sci. USA* 96, 11883–11888.
- Hariharan, I.K., 2015. Organ size control: lessons from *Drosophila*. *Dev. Cell* 34, 255–265.
- Haynie, J., Bryant, P., 1977. The effects of X-rays on the proliferation dynamics of cells in the imaginal wing disc of *Drosophila melanogaster*. *Roux's Arch. Dev. Biol.* 183, 85–100.
- Holloway, D.M., Lopes, F.J., da Fontoura Costa, L., Travencolo, B.A., Golyandina, N., Usevich, K., Spirov, A.V., 2011. Gene expression noise in spatial patterning: hunchback promoter structure affects noise amplitude and distribution in *Drosophila* segmentation. *PLoS Comput. Biol.* 7, e1001069.
- Holtzinger, A., Evans, T., 2005. *Gata4* regulates the formation of multiple organs. *Development* 132, 4005–4014.
- Hunter, C.P., Kenyon, C., 1996. Spatial and temporal controls target *pal-1* blastomere-specification activity to a single blastomere lineage in *C. elegans* embryos. *Cell* 87, 217–226.
- Irvine, K.D., Harvey, K.F., 2015. Control of organ growth by patterning and hippo signaling in *Drosophila*. *Cold Spring Harb. Perspect. Biol.*, 7. <http://dx.doi.org/10.1101/cshperspect.a019224>, pii: a019224.
- Kostic, I., Roy, R., 2002. Organ-specific cell division abnormalities caused by mutation in a general cell cycle regulator in *C. elegans*. *Development* 129, 2155–2165.

- Lee, Y.U., Son, M., Kim, J., Shim, Y.H., Kawasaki, I., 2016. CDC-25.2, a *C. elegans* ortholog of *cdc25*, is essential for the progression of intestinal divisions. *Cell Cycle* 15, 654–666.
- Lemaitre, B., Miguel-Aliaga, I., 2013. The digestive tract of *Drosophila melanogaster*. *Annu. Rev. Genet.* 47, 377–404.
- Leung, B., Hermann, G.J., Priess, J.R., 1999. Organogenesis of the *Caenorhabditis elegans* intestine. *Dev. Biol.* 216, 114–134.
- Lin, R., Thompson, S., Priess, J.R., 1995. *pop-1* encodes an HMG box protein required for the specification of a mesoderm precursor in early *C. elegans* embryos. *Cell* 83, 599–609.
- Maduro, M.F., 2009. Structure and evolution of the *C. elegans* embryonic endomesoderm network. *Biochim. Biophys. Acta* 1789, 250–260.
- Maduro, M.F., 2015. Developmental robustness in the *Caenorhabditis elegans* embryo. *Mol. Reprod. Dev.* 918–931.
- Maduro, M.F., 2017. Gut development in *C. elegans*. *Semin. Cell Dev. Biol.* <http://dx.doi.org/10.1016/j.semcdb.2017.01.001>.
- Maduro, M.F., Meneghini, M.D., Bowerman, B., Broitman-Maduro, G., Rothman, J.H., 2001. Restriction of mesendoderm to a single blastomere by the combined action of SKN-1 and a GSK-3 β homolog is mediated by MED-1 and -2 in *C. elegans*. *Mol. Cell* 7, 475–485.
- Maduro, M.F., Hill, R.J., Heid, P.J., Newman-Smith, E.D., Zhu, J., Priess, J., Rothman, J., 2005a. Genetic redundancy in endoderm specification within the genus *Caenorhabditis*. *Dev. Biol.* 284, 509–522.
- Maduro, M.F., Kasmir, J.J., Zhu, J., Rothman, J.H., 2005b. The Wnt effector POP-1 and the PAL-1/Caudal homeoprotein collaborate with SKN-1 to activate *C. elegans* endoderm development. *Dev. Biol.* 285, 510–523.
- Maduro, M.F., Broitman-Maduro, G., Mengarelli, I., Rothman, J.H., 2007. Maternal deployment of the embryonic SKN-1 –> MED-1,2 cell specification pathway in *C. elegans*. *Dev. Biol.* 301, 590–601.
- Maduro, M.F., Broitman-Maduro, G., Choi, H., Carranza, F., Chia-Yi Wu, A., Rifkin, S.A., 2015. MED GATA factors promote robust development of the *C. elegans* endoderm. *Dev. Biol.* 404, 66–79.
- Mann, F.G., Van Nostrand, E.L., Friedland, A.E., Liu, X., Kim, S.K., 2016. Deactivation of the GATA transcription factor ELT-2 is a major driver of normal aging in *C. elegans*. *PLoS Genet.* 12, e1005956.
- McGhee, J.D., Fukushige, T., Krause, M.W., Minnema, S.E., Goszczynski, B., Gaudet, J., Kohara, Y., Bossinger, O., Zhao, Y., Khattra, J., Hirst, M., Jones, S.J., Marra, M.A., Ruzanov, P., Warner, A., Zapf, R., Moerman, D.G., Kalb, J.M., 2009. ELT-2 is the predominant transcription factor controlling differentiation and function of the *C. elegans* intestine, from embryo to adult. *Dev. Biol.* 327, 551–565.
- Murray, J.I., Bao, Z., Boyle, T.J., Boeck, M.E., Mericle, B.L., Nicholas, T.J., Zhao, Z., Sandel, M.J., Waterston, R.H., 2008. Automated analysis of embryonic gene expression with cellular resolution in *C. elegans*. *Nat. Methods* 5, 703–709.
- Okumura, T., Matsumoto, A., Tanimura, T., Murakami, R., 2005. An endoderm-specific GATA factor gene, dGATAe, is required for the terminal differentiation of the *Drosophila* endoderm. *Dev. Biol.* 278, 576–586.
- Owraghi, M., Broitman-Maduro, G., Luu, T., Roberson, H., Maduro, M.F., 2010. Roles of the Wnt effector POP-1/TCF in the *C. elegans* endomesoderm specification gene network. *Dev. Biol.* 340, 209–221.
- Palgunow, D., Klapper, M., Doring, F., 2012. Dietary restriction during development enlarges intestinal and hypodermal lipid droplets in *Caenorhabditis elegans*. *PLoS One* 7, e46198.
- Patel, S.H., Camargo, F.D., Yimlamai, D., 2017. Hippo signaling in the liver regulates organ size, cell fate, and carcinogenesis. *Gastroenterology* 152, 533–545.
- Praitis, V., Casey, E., Collar, D., Austin, J., 2001. Creation of low-copy integrated transgenic lines in *Caenorhabditis elegans*. *Genetics* 157, 1217–1226.
- Raj, A., Rifkin, S.A., Andersen, E., van Oudenaarden, A., 2010. Variability in gene expression underlies incomplete penetrance. *Nature* 463, 913–918.
- Rasmussen, J.P., Feldman, J.L., Reddy, S.S., Priess, J.R., 2013. Cell interactions and patterned intercalations shape and link epithelial tubes in *C. elegans*. *PLoS Genet.* 9, e1003772.
- Rehorn, K.P., Thelen, H., Michelson, A.M., Reuter, R., 1996. A molecular aspect of hematopoiesis and endoderm development common to vertebrates and *Drosophila*. *Development* 122, 4023–4031.
- Reuter, R., 1994. The gene *serpent* has homeotic properties and specifies endoderm versus ectoderm within the *Drosophila* gut. *Development* 120, 1123–1135.
- Robertson, S.M., Medina, J., Lin, R., 2014. Uncoupling different characteristics of the *C. elegans* E lineage from differentiation of intestinal markers. *PLoS One* 9, e106309.
- Ryoo, H.D., Bergmann, A., 2012. The role of apoptosis-induced proliferation for regeneration and cancer. *Cold Spring Harb. Perspect. Biol.* 4, a008797.
- Sarov, M., Schneider, S., Pozniakovski, A., Roguev, A., Ernst, S., Zhang, Y., Hyman, A.A., Stewart, A.F., 2006. A recombining pipeline for functional genomics applied to *Caenorhabditis elegans*. *Nat. Methods* 3, 839–844.
- Shetty, P., Lo, M.C., Robertson, S.M., Lin, R., 2005. *C. elegans* TCF protein, POP-1, converts from repressor to activator as a result of Wnt-induced lowering of nuclear levels. *Dev. Biol.* 285, 584–592.
- Sommermann, E.M., Strohmaier, K.R., Maduro, M.F., Rothman, J.H., 2010. Endoderm development in *Caenorhabditis elegans*: the synergistic action of ELT-2 and -7 mediates the specification –> differentiation transition. *Dev. Biol.* 347, 154–166.
- Sulston, J.E., Horvitz, H.R., 1977. Post-embryonic cell lineages of the nematode, *Caenorhabditis elegans*. *Dev. Biol.* 56, 110–156.
- Sulston, J.E., Schierenberg, E., White, J.G., Thomson, J.N., 1983. The embryonic cell lineage of the nematode *Caenorhabditis elegans*. *Dev. Biol.* 100, 64–119.
- Tamori, Y., Deng, W.M., 2014. Compensatory cellular hypertrophy: the other strategy for tissue homeostasis. *Trends Cell Biol.* 24, 230–237.
- Wehman, A.M., Poggioli, C., Schweinsberg, P., Grant, B.D., Nance, J., 2011. The P4-ATPase TAT-5 inhibits the budding of extracellular vesicles in *C. elegans* embryos. *Curr. Biol.* 21, 1951–1959.
- Wiesenfahrt, T., Berg, J.Y., Nishimura, E.O., Robinson, A.G., Goszczynski, B., Lieb, J.D., McGhee, J.D., 2015. The function and regulation of the GATA Factor ELT-2 in the *C. elegans* endoderm. *Development* 143, 483–491.
- Zaret, K.S., 2016. From Endoderm to Liver Bud: paradigms of Cell Type Specification and Tissue Morphogenesis. *Curr. Top. Dev. Biol.* 117, 647–669.
- Zhu, J., Hill, R.J., Heid, P.J., Fukuyama, M., Sugimoto, A., Priess, J.R., Rothman, J.H., 1997. *end-1* encodes an apparent GATA factor that specifies the endoderm precursor in *Caenorhabditis elegans* embryos. *Genes Dev.* 11, 2883–2896.
- Zhu, J., Fukushige, T., McGhee, J.D., Rothman, J.H., 1998. Reprogramming of early embryonic blastomeres into endodermal progenitors by a *Caenorhabditis elegans* GATA factor. *Genes Dev.* 12, 3809–3814.